02,12

Influence of intragranular Meissner currents and magnetic flux trapped in granules on the effective field in the intergranular medium and the magnetoresistance hysteresis of a granular HTSC

© D.A. Balaev, S.V. Semenov, D.M. Gokhfeld

Kirensky Institute of Physics, Federal Research Center KSC SB, Russian Academy of Sciences, Krasnoyarsk, Russia

E-mail: dabalaev@iph.krasn.ru

Received July 18, 2022
Revised July 18, 2022
Accepted July 19, 2022

The concept of an effective field in an intergranular medium is used to describe the hysteresis magnetoresistance of granular HTSCs. This effective field is a superposition of the external magnetic field and the field induced by the magnetic moments of the superconducting granules. The magnetic moment of the granules is contributed by the shielding currents and the trapped magnetic flux. We studied and analyzed the effect of the trapped flux on the magnetoresistance. It has been experimentally shown that the dependence of the residual resistance R_{Rem} (after applying of the external field) on the trapped flux clearly correlates with the behavior of the remanent magnetization. In addition, special attention was paid to a detailed comparison of the magnetoresistance of the granular $YBa_2Cu_3O_{7-\delta}$ for two cases: (a) the magnetization of HTSC-granules is caused only by the trapped magnetic flux (in a zero external field) and (b) HTSC-granules are in the Meissner state (the external field is smaller than the first critical field of the granules). It has been found that Abrikosov vortices and intragranular Meissner currents differently affect the effective field in the intergranular medium (for the same values (of magnetization for cases (a) and (b)). A possible reason for this difference is discussed.

Keywords: granular HTSC, magnetoresistance hysteresis, magnetization hysteresis, trapped flux, screening currents.

DOI: 10.21883/PSS.2022.12.54376.442

1. Introduction

Studies of magnetotransport properties of the obtained superconducting materials are an integral part of their characterization [1–15]. This applies both to the already „classical“, granular high-temperature superconductors (HTS), and new, „hydride“ superconductors [13,14]. The short coherence length inherent in superconductors with a high critical temperature causes nontrivial effects associated with the granularity of the material. If the coherence length is comparable to the size of the area separating the granules, in fact, with the length of the intergranular boundary, then a connection is formed between the granules through the Josephson effect. In this case, a granular superconductor can be represented as a two-level superconducting system [15], in which „is a strong superconductor“ — these are HTS granules, and „is a weak superconductor“ — a subsystem of intergranular boundaries (in fact, weak Josephson-type bonds).

For HTS classical compositions — yttrium, bismuth and lanthanum, such a two-level superconducting properties are known [15–21]. To date, a model has been proposed that explains the totality of the magnetotransport properties of [21–29], which at first glance are difficult to explain. It is possible to note a series of recent works in which features of the behavior of the electrical resistance of granular Y–Ba–Cu–O in external fields were discovered, indicating the course of the Berezinsky–Kosterlitz–Taules topological phase transition in the intergranular medium [30–34]. For some low-temperature superconductors, effects related to the Josephson coupling between superconducting granules [35–37], or superconducting areas, are also observed [38], and, as a consequence, with the implementation of a two-level superconducting system. In the study [39], a purposeful search for hysteresis effects in the behavior of magnetoresistance of „hydride“ superconductors that can maintain superconductivity to temperatures near room temperature under high pressures was proposed [13,14].

The description of hysteresis effects in the magnetotransport properties of granular superconductors is based on the concept of an effective field in an intergranular medium [21–29,40,41]. This effective field $\mathbf{B}_{\mathrm{eff}}$ is a superposition of the external field $\mathbf{H}$ and the field $\mathbf{B}_{\mathrm{ind}}$ induced by magnetic moments of HTS granules [21–29]. Here we can draw some analogy with the Weiss molecular field for ferromagnets. And similarly to the Weiss molecular field, the field $\mathbf{B}_{\mathrm{ind}}$ in an intergranular medium is also associated with the magnetization of a superconductor $M(H)$, which, as a result, gives the following expression for the effective field $\mathbf{B}_{\mathrm{eff}}$ [21–29]:

$$\mathbf{B}_{\mathrm{eff}}(\mathbf{H}) = \mathbf{H} + 4\pi \cdot \alpha \cdot \mathbf{M}(\mathbf{H}). \quad (1)$$

The α parameter in the expression (1) includes both the averaged demagnetizing factor of the granule shape and the effect of compression of the magnetic flux in the intergranular medium [23,25–29]. The compression of the magnetic flux in an intergranular medium was first mentioned in the work [42]. Later, in a number of works, the degree of compression of the magnetic flux was quantified (the value of the parameter was obtained α, which numerically amounted to 12÷25) [23,25–29], and it is shown that it is taking into account the compression of the flux that allows us to qualitatively and even, in some cases, quantitatively describe the experimentally observed dependences of magnetoresistance [43].

The magnetization (magnetization curve) of a superconductor is determined by two contributions — Abrikosov vortices (trapped flux) and Meissner currents (diamagnetic signal). The amount of trapped flux is determined by the value of the maximum applied external field $H_{\max}$ and the thermomagnetic background. After the input/output of the external field (at $H = 0$), the magnetization of the superconductor is determined only by the trapped flux, and the superconductor has a residual magnetization of M_{Rem}. At the same time, a fully diamagnetic state (without magnetic flux capture) is realized in a range of relatively small external fields. In order to further develop a model explaining hysteresis effects in the magnetotransport properties of granular superconductors, the correlation between the values of the residual resistance R_{Rem} (at $H = 0$ after input/output of the external field) and the residual magnetization M_{Rem} is investigated in this paper. Also, we propose a method for experimentally determining the relationship between the parameters α for Meissner currents and for Abrikosov vortices. To achieve this goal, this work analyzes and compares the magnitudes of the magnetoresistance of a granular HTS $YBa_2Cu_3O_{7-\delta}$ (a) in a state of residual magnetization, with a variable the amount of trapped flux and (b) in the fully Meissner state of superconducting granules.

2. Experiment

The studied HTS sample $YBa_2Cu_3O_{7-\delta}$ was prepared by solid-phase synthesis from the corresponding oxides with three intermediate grinds. The diffractogram of the obtained sample showed only reflexes corresponding to the structure 1−2−3. According to the results of scanning electron microscopy (the data were obtained using a Hitachi-TM 4000 electron microscope), the average size of the granules was 5 μm [44].

Electrical resistance R was measured by the four-probe method; the sample dimensions were $0.8\times0.8\times6\,\text{mm}^3$. When measuring $R(H)$, the sample was in a liquid nitrogen medium, which provided effective removal of the released heat and allowed us to obtain $R(H)$ dependences in the transport current of 300 mA without the influence of the Joule heating effect. The external field perpendicular to the direction of the transport current was set by an electromagnet. Part of the measurements of temperature dependences $R(T)$ were carried out using the PPMS-9T setup (under cooling conditions in a zero external field). We need to distinguish two types of dependencies $R(H)$: (1) after cooling in a zero external field, when the field increases, the initial magnetoresistance curve $R(H_{\text{ini}})$ is measured, (2) after cooling without a field, the external field increases to a certain maximum value $H_{\max}$, and then cycles within $\pm H_{\max}$; then $|H_{\max}|$ increases by some amount and the field cycles again within $\pm H_{\max}$, and so on. For the case (2) a family of hysteresis loops $R(H)$ was obtained at various values $|H_{\max}|$. The rate of change of the external field was constant and was 1 Oe/s.

Magnetic properties of (dependences of $M(H)$ and $M(T)$) were measured on a LakeShore VSM 8604 vibration magnetometer on the same HTS sample on which $R(H)$ measurements were carried out. The temperature (77.4 K), the scanning speed of the external magnetic field, the measurement modes and the mutual configuration of the geometric dimensions of the sample and the external field were identical to the magnetoresistance measurements.

3. Results and discussion

3.1. Illustration of the implementation of a two-level superconducting system of the investigated granular HTS based on its magnetotransport properties

According to magnetic measurements, the temperature of the transition to the superconducting state of the studied sample was 92.8 K, and at the same temperature, the beginning of the resistive transition is observed (Fig. 1, a). The value of the critical current density at $T = 77.4$ K in the zero external field was $\sim 80\,\text{A/cm}^2$. These results are typical for granular HTS with the structure 1−2−3.

Fig. 1 shows the dependences of resistance on temperature $R(T)$ in various external fields (a) and magnetoresistance $R(H)$ (b). A sharp jump in resistance corresponds to a superconducting transition in HTS granules, and the tightened part of the resistive transition, manifested even in sufficiently weak external fields, corresponds to a transition in the intergranular boundaries (Fig. 1, a). A similar „two-stage“ dissipation modes is also manifested in the dependencies $R(H)$, see Fig. 1, b. With an increase in the field, the resistance first increases quite sharply, and then, it goes to the „intermediate plateau“. With a further increase in the external field, the resistance begins to increase again. Based on this, we can talk about two modes of dissipation. In the first mode, dissipation occurs only in the intergranular boundaries (the area of relatively low fields), in the second mode (the area of large fields), dissipation occurs already in granules, and the intergranular boundaries are completely in a resistive state. Experimental data in Fig. 1 allow us to determine the interface between the specified dissipation modes. These boundaries are designated as horizontal point

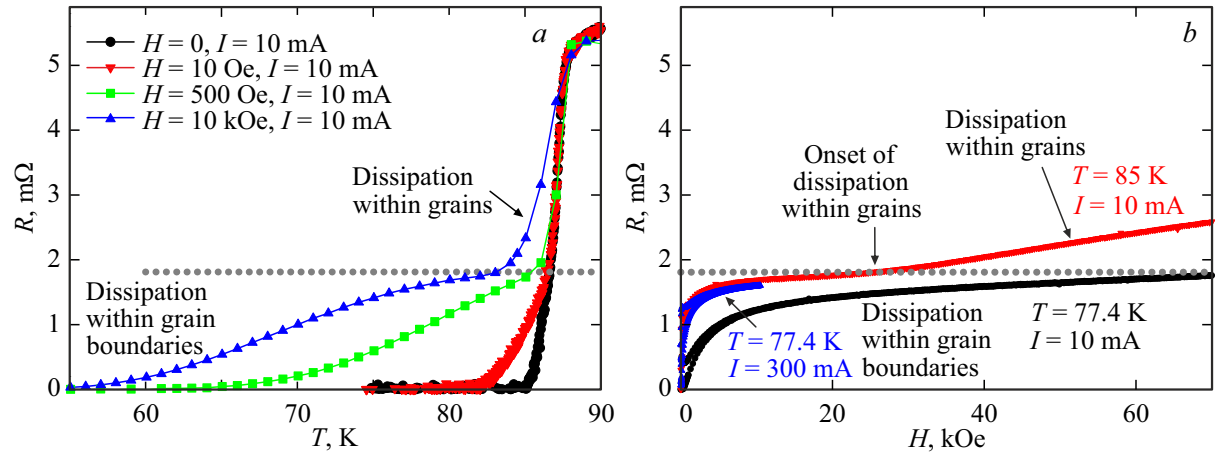

Figure 1. Magnetotransport properties (dependencies $R(T)$ — (a) and $R(H)$ —(b)) of the studied sample of granular $YBa_2Cu_3O_{7-\delta}$. The experimental conditions (external field H and transport current I, temperature values T) are indicated in the field of the figure. Dotted horizontal lines on (a) and (b) delimit the areas where dissipation occurs only in the intergranular space (from below) and in granules and intergranular space (from above).

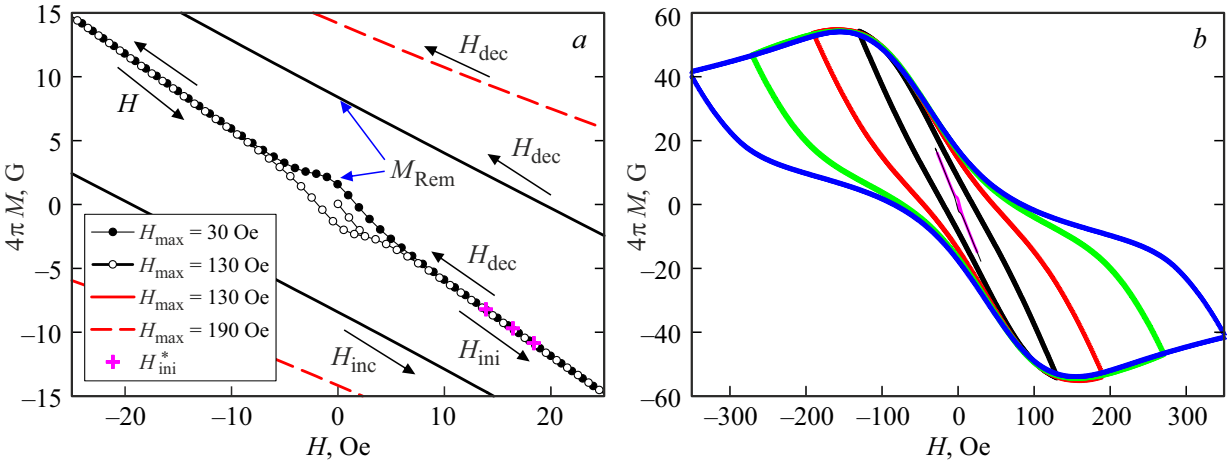

Figure 2. Typical magnetic hysteresis loops $M(H)$ for the studied sample $YBa_2Cu_3O_{7-\delta}$ at $T = 77.4$ K, obtained up to various values of the maximum applied fields H_{max}. (a) — zoomed in the neighborhood of $H = 0$ (the values of H_{max} are specified in the legend), (b) — full scale. The arrows on (a) show the direction of change of the external field, and also denotes the increasing H_{inc} (H_{ini} — for the initial magnetization curve), decreasing H_{dec} fields and residual magnetization M_{Rem}; also points $M(H^*_{ini})$ are specified for comparison with the dependence $R(H_{ini})$, see the text.

lines (the scales along the resistance axis are the same in Fig. 1, a and 1, b), which illustrates the implementation of a two-level superconducting system in a granular HTS. The analysis of the hysteresis dependences of $R(H)$ carried out below corresponds to a mode in which dissipation occurs only in the intergranular boundaries.

3.2. Magnetic hysteresis loops: a manifestation of a two-level superconducting system and a condition for the realization of the Meissner state of HTS granules

Fig. 2, a shows the parts of the dependencies $M(H)$ of the studied sample obtained up to different values $|H_{max}|$. For data at $|H_{max}| = 30$ Oe, hysteresis is visible in the field area up to about ± 8 Oe, and in the range of fields larger than this value, the dependence of $M(H)$ becomes an invertible function linearly dependent on the external field. Hysteresis in the area of small fields is obviously caused by a response from the subsystem of intergranular boundaries, and in the specified range ± 8 Oe, a complete shielding of the external field occurs throughout the sample. We note that the described „small“ hysteresis was observed on granular HTS earlier [45–47].

With an increase in the external field, the magnetic flux begins to penetrate into the HTS-granules. The magnetic flux trapping in the granules leads to the appearance of a pronounced hysteresis of the dependencies $M(H)$,

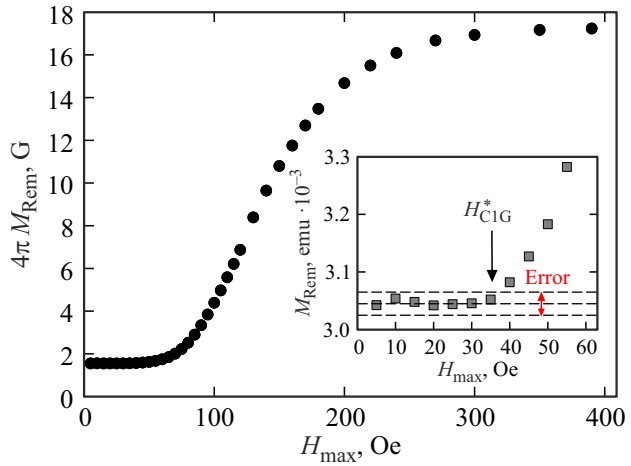

Figure 3. Dependence of the residual magnetization M_{Rem} on the maximum applied field H_{max}. In the insert: the behavior of $M_{\text{Rem}}(H_{\text{max}})$ in absolute units of magnetization (emu) with an indication of an instrumental error; the field H^*_{C1G} is specified, see the text.

see Fig. 2, *b*. At the same time, the „small" hysteresis becomes almost indistinguishable (Fig. 2, *b*). This behavior of magnetization (two different hysteresis values $M(H)$) is a manifestation of a two-level superconducting system in granular HTS. We also note that the $M(H)$ dependences shown in Fig. 2, *b* are typical for granular HTS in the area of sufficiently high temperatures [48–50], and the asymmetry of the magnetization hysteresis loops relative to the abscissa axis is explained by the weakening of the pinning of Abrikosov vortices in the near-surface the layer of granules [48–50].

For granular (or polycrystalline) HTS, instead of the first critical field H_{C1}, it is more appropriate to use the term „the first field of penetration" H^*_{C1G} into granules [51,52]. To determine this field, it is advisable to consider the behavior of the residual magnetization M_{Rem} (an example of determining M_{Rem} is shown in Fig. 2, *a*), as a function of the maximum applied field H_{max}, see fig. 3. From this figure it can be seen that the dependence $M_{\text{Rem}}(H_{\text{max}})$ has a characteristic S-shaped appearance; the output to the plateau at values of H_{max}, about 300−400 Oe, is due to the fact that at these values H_{max}, the position of the dependence $M(H)$ in the vicinity of the origin becomes close for the limit hysteresis loop. A nonzero value of M_{Rem} with small values of H_{max} is a manifestation of „of small hysteresis" from the subsystem of intergranular boundaries (see Fig. 2, *a*). The insert of Fig. 3 illustrates the behavior of $M_{\text{Rem}}(H_{\text{max}})$ in the area of small fields; here the data is given in units of emu. Horizontal dashed lines show the instrumental error ($\pm 2 \cdot 10^{-5}$ emu). From the insert of Fig. 3, it can be seen that the dependence of $M_{\text{Rem}}(H_{\text{max}})$ on a constant value occurs in the neighborhood of $H_{\text{max}} \approx 35$ Oe. Logically, this value of the external field can be considered the field of the first penetration of H^*_{C1} into the granules of the HTS. In the field range, at least up to 35 Oe, only the Meissner state is realized in the HTS granules, and there is no flax trapping.

3.3. Hysteresis $R(H)$ and effect of the magnitude H_{max} on residual resistance R_{Rem}

Fig. 4, *a* shows both the initial magnetoresistance curve $R(H_{\text{ini}})$ and the dependence $R(H)$ obtained by cycling the external field to the value $H_{\text{max}} = \pm 310$ Oe. This figure shows the relative position of $R(H_{\text{ini}})$ and branches of the descending $R(H_{\text{dec}})$ and increasing $R(H_{\text{inc}})$ fields. The dependence of $R(H)$ when cycling the field is symmetric with respect to the ordinate axis. The intersection point of $R(H_{\text{d}})$ and $R(H_{\text{inc}})$ is at $H = 0$, and this is — the residual resistance of R_{Rem} after the input/output of the field. Fig. 4, *b* shows a family of dependencies $R(H)$ obtained by cycling the external field to various values H_{max} (this figure shows mainly the positive area of the external field). It can be seen that with an increase in H_{max}, the value of the residual resistance of R_{Rem} increases. In our experiment, magnetoresistance loops were measured for various values of H_{max}, and the dependence of R_{Rem} on H_{max} obtained from the experimental data set is shown in Fig. 5, *a*.

Dependencies $R_{\text{Rem}}(H_{\text{max}})$ in Fig. 5, *a*, as well as dependencies $R(H)$ in Fig. 4 correspond to the mode in which dissipation occurs only in an intergranular environment. This can be seen from the comparison of the data in Fig. 4 and Fig. 1, *b*: a multiple increase in current (from 10 to 300 mA) does not lead to dissipation in granules and the dependence $R(H)$ is inside the area corresponding to dissipation only in the intergranular boundaries.

3.4. The concept of an effective field in the intergranular medium of a granular HTS

According to the concept of the effective field in the intergranular medium of granular HTS, the observed magnetoresistance is determined by the value of the effective field B_{eff} (see Introduction). Based on the results obtained above, let us consider the case when all dissipation (nonzero resistance) occurs only in an intergranular medium, and the state with „zero" resistance is preserved in the granules. Expression (1) is written in vector form, and in order to move to the value of B_{eff}, it is necessary to consider the relative position of the magnetic induction lines from the magnetic moments of the HTS granules and the direction of the external field, see Fig. 6. In this schematic representation, the magnetic moments of the HTS granules are considered $\mathbf{M}_{\text{G}}$ ($\Sigma \mathbf{M}_{\text{G}} = \mathbf{M}_{\text{tot}}$, projection $\mathbf{M}_{\text{tot}}$ on the axis $\mathbf{Z}$ — this is the magnetic moment of the entire sample). When the outer field increases ($H = H_{\text{inc}}$, $\mathbf{H} = \mathbf{H}_Z$), $\mathbf{M}_{\text{G}}$ are directed against the outer field ($\mathbf{M}_{\text{GZ}} = |\mathbf{M}_{\text{G}}|$), and this situation corresponds to the negative values of magnetization in Fig. 2. In this case, the magnetic induction lines from $\mathbf{M}_{\text{G}}$ in the area of the boundary between the granules are co-directed to the external field, see Fig. 6 (dashed lines). If at $H = H_{\text{dec}}$ the

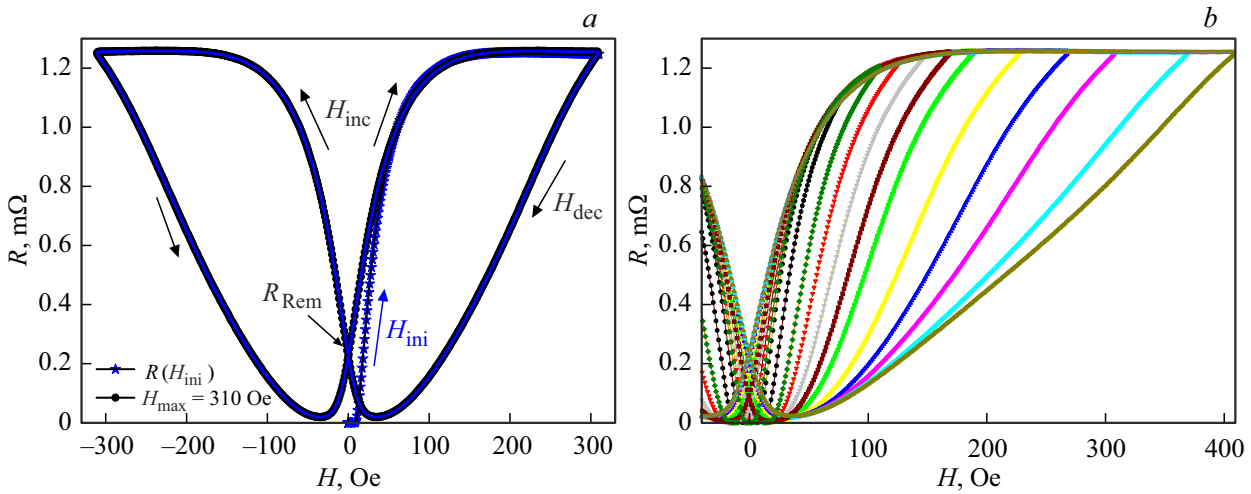

Figure 4. (a) — the initial magnetoresistance curve $R(H_{ini})$ and the hysteresis dependence $R(H)$, when the external field changes to $H_{max} = \pm 310$ Oe. The arrows show the direction of the field change, the symbols of the increasing H_{inc} and decreasing H_{dec} fields are given, as well as the residual resistance R_{Rem}, (b) — sections of magnetoresistance loops when cycling to different field values $\pm H_{max}$.

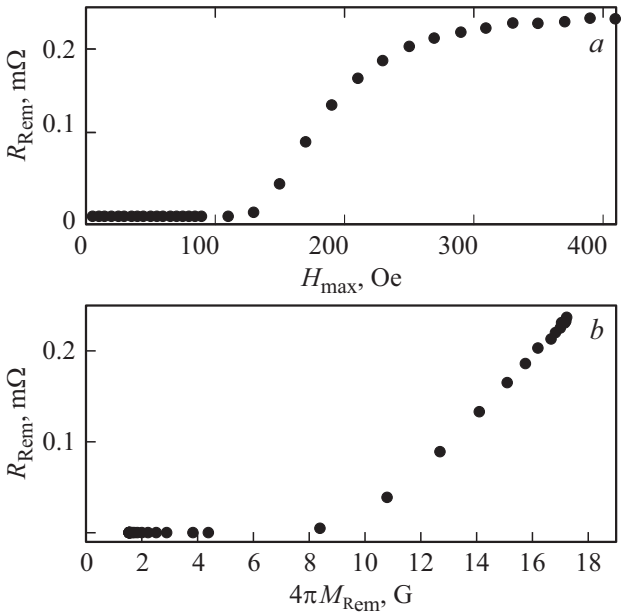

Figure 5. Residual resistance R_{Rem} depending on the external field (a) and the residual magnetization (b).

magnetization values take positive values (the first quadrant of Fig. 2), then $\mathbf{M}_{GZ} = |\mathbf{M}_G|$ and $\mathbf{M}_{GZ} \parallel \mathbf{H}$. In this case, the directions of the vectors $\mathbf{M}_G$ and the magnetic induction lines shown in Fig. 6 will change to the opposite (they will be directed against the external field). The above allows you to rewrite the expression (1) in scalar form, as $B_{eff}(H) = H - 4\pi \cdot \alpha M(H)$. Since the magnetoresistance of a superconductor is — an even function of the magnetic field, it is necessary to take the effective field modulus, which leads to the following expression

$$B_{eff}(H) = |H - 4\pi \cdot \alpha \cdot M(H)|. \qquad (2)$$

We note that the density of the magnetic induction lines in the space between the granules visible in Fig. 6 reflects the effect of compression of the flux in the intergranular medium of granular HTS, which manifests itself in large values of the parameter α required to describe the experimental hysteresis of magnetoresistance [23,25–29,43,44]. As for the transition from the effective field to the electrical resistance, R is a function of B_{eff}, which is a function of the field: $R = f\left(B_{eff}(H)\right)$. The function f — is usually an Arrhenius-type expression operating with the ratio of pinning energy (or Josephson coupling energy) and thermal energy [53,54].

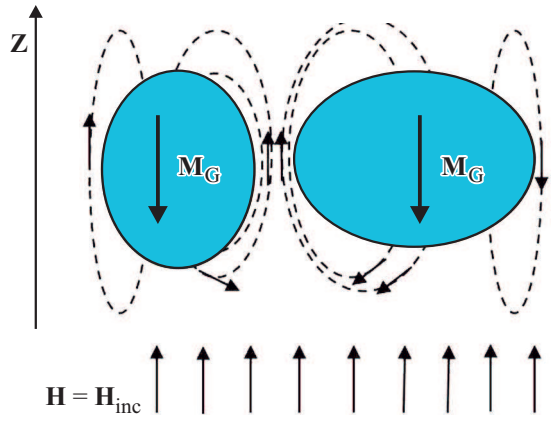

Figure 6. Schematic representation of the mutual direction relative to the axis **Z**, along which an increasing external field $\mathbf{H}_{inc}$ is applied, of the magnetic moments $\mathbf{M}_G$ of two adjacent HTS-granules, as well as magnetic induction lines (dashed lines) from $\mathbf{M}_G$. Granules are shown as ovals, the space between them is — the intergranular boundary (in real granular HTS-granules have micron sizes, and the thickness of the intergranular boundaries is on the order of nanometers).

3.5. Relationship of residual resistance R_{Rem} and residual magnetization M_{Rem}

Let us return to the consideration of the residual resistance R_{Rem} (Fig. 4, 5, *a*). With some degree of conditionality, the dependence $R_{\mathrm{Rem}}(H_{\max})$, shown in Fig. 5, *a*, is similar to the dependence $M_{\mathrm{Rem}}(H_{\max})$ in Fig. 4. Comparing the data of Fig. 4 and Fig. 5, *a*, it can be noted that both dependencies are $M_{\mathrm{Rem}}(H_{\max})$ and $R_{\mathrm{Rem}}(H_{\max})$ show a tendency to saturation. For the conditions of residual magnetization and (or) residual resistance, the expression (2) will be rewritten in the following form

$$B_{\mathrm{eff\,Rem}} = 4\pi \cdot \alpha \cdot M_{\mathrm{Rem}}. \qquad (3)$$

This expression explains the same tendency to saturation of the dependencies $R_{\mathrm{Rem}}(H_{\max})$ and $M_{\mathrm{Rem}}(H_{\max})$, given that the resistance — is a function of the effective fields $R \sim f(B_{\mathrm{eff}})$. Fig. 5, *b* shows the dependence of R_{Rem} on M_{Rem} obtained with the same values of $H_{\max}$. Zero resistance values up to the value of $4\pi \cdot M_{\mathrm{Rem}} \approx 8\,\mathrm{Gs}$ are determined by the fact that the transport current in this case is less than the value of the intergranular critical current. With a further increase in the value of the trapped flux, the effective field in the intergranular medium ($B_{\mathrm{eff\,Rem}}$ — expression (3)) is growing, and this leads to a monotonous growth of R_{Rem} in accordance with the consideration of [53] dissipation processes. Thus, the data in Fig. 5, *b*, in fact, represent the initial dependence of the resistance of the intergranular medium on the magnitude of the magnetization of the granules, and the latter is determined only by the flux trapped inside the granules (Abrikosov vortices).

3.6. Justification of the method for determining the parameter α for Meissner currents and Abrikosov vortices

If in Section 3.5 the state in which the magnetization of granules is determined only by the trapped flux was considered, then in external fields up to the value of H^*_{C1G} ($\approx 35\,\mathrm{Oe}$ for $T = 77.4\,\mathrm{K}$, see clause 3.2 and Fig. 2) only the Meissner state is realized in the granules (when cooled in a zero external field). This case corresponds to the initial magnetization curve $M(H_{\mathrm{ini}})$, or, in the case of magnetoresistance — dependence $R(H_{\mathrm{ini}})$.

In expressions (1) and (2), the parameter α is, in fact, the coefficient of proportionality between the magnetization of granules (in the corresponding system of units) and the field induced into the intergranular medium. Our idea is to compare the effective fields for two different states in the HTS granules: the Meissner state (while there are no Abrikosov vortices in the granules) and for the trapped flux state (while there are no Meissner currents in the granules). Comparison of effective fields for the specified states will be valid for the same resistance value $R = \mathrm{const}$ in them, since this condition is equivalent to the condition $B_{\mathrm{eff}} = \mathrm{const}$.

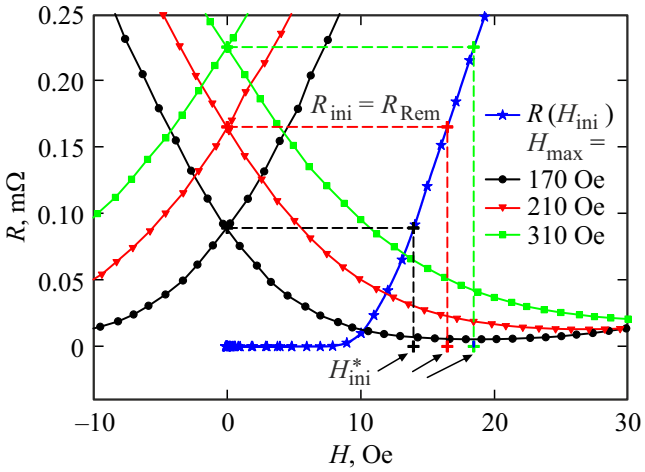

Figure 7. A plot of hysteresis dependencies $R(H)$ near $H = 0$ at various specified values of the maximum applied field $H_{\max}$. Horizontal dashed lines correspond to the condition $R_{\mathrm{Rem}} = R(H^*_{\mathrm{ini}})$. The definition of the values of H^*_{ini} is also shown.

Fig. 7, on an enlarged scale in a range of small external fields, shows both the dependency $R(H_{\mathrm{ini}})$ and the dependency sections $R(H_{\mathrm{inc}})$, $R(H_{\mathrm{dec}})$ with sample values of $H_{\max}$ (shown in the figure). The horizontal segments in Fig. 7 are drawn from the values of R_{Rem} to their intersection with the dependency $R(H_{\mathrm{ini}})$ to illustrate the condition $R_{\mathrm{Rem}} = R_{\mathrm{ini}}$ and explanations of finding the values of H^*_{ini}, in which $R_{\mathrm{Rem}} = R(H^*_{\mathrm{ini}})$. The condition $R_{\mathrm{Rem}} = R_{\mathrm{ini}}(H^*_{\mathrm{ini}})$ is equivalent to the condition of equality of effective fields

$$B_{\mathrm{eff\,Rem}} = B_{\mathrm{eff}}(H^*_{\mathrm{ini}}). \qquad (4)$$

$B_{\mathrm{eff\,Rem}}$ is determined only by the value of the residual magnetization (expression (3)). The effective field $B_{\mathrm{eff}}(H^*_{\mathrm{ini}})$ for the initial dependence of the magnetoresistance, according to the expression (2), will be defined as

$$B_{\mathrm{eff}}(H^*_{\mathrm{ini}}) = |H^*_{\mathrm{ini}} - 4\pi \cdot \alpha \cdot M(H^*_{\mathrm{ini}})|. \qquad (5)$$

The values of $M(H^*_{\mathrm{ini}})$ are contained in the magnetization data in Fig. 2, *a*, and the same figure shows the points of dependence of $M(H^*_{\mathrm{ini}})$ with values of H^*_{ini} corresponding to Fig. 7. We note that all the obtained values of H^*_{ini} lie in the range $9 \div 20\,\mathrm{Oe}$, which corresponds to the Meissner state of the HTS granules.

Now, instead of one common parameter α, we introduce the parameters α_{A} and α_{M}, characterizing the condensation of magnetic induction lines only from Abrikosov vortices and only from Meissner currents, respectively. As a result, based on (3) and (5), the condition of equality of effective fields (4) can be written as

$$4\pi \cdot \alpha_{\mathrm{A}} \cdot M_{\mathrm{Rem}} = H^*_{\mathrm{ini}} - 4\pi \cdot \alpha_{\mathrm{M}} \cdot M(H^*_{\mathrm{ini}}). \qquad (6)$$

In our experiment, magnetoresistance loops were measured for 15-th different values of $H_{\max}$, at which analysis can be carried out within the expression (6) (it is necessary

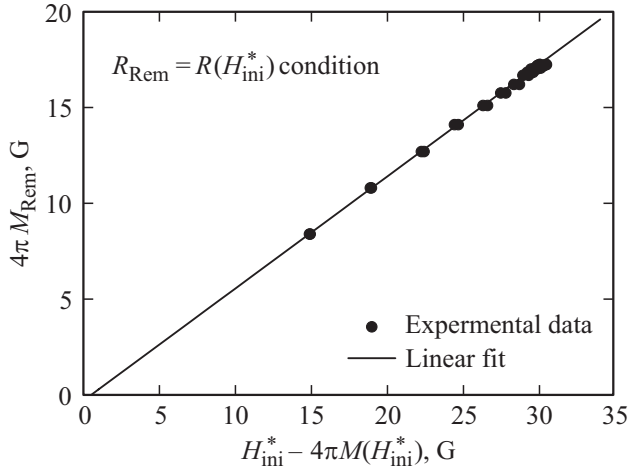

Figure 8. Experimental values of $4\pi \cdot M_{\mathrm{Rem}}$ from $(H^*_{\mathrm{ini}} - 4\pi \cdot M(H^*_{\mathrm{ini}})$, defined by the condition $R_{\mathrm{Rem}} = R(H^*_{\mathrm{ini}})$, see Fig. 8.

that in the state after the input/output of the field, the sample demonstrates a non-zero value R_{Rem}). Experimental values of $4\pi \cdot M_{\mathrm{Rem}}$ and $(H^*_{\mathrm{ini}} - 4\pi \cdot M(H^*_{\mathrm{ini}}))$ are shown in Fig. 8, from which it can be seen that they obey a linear dependence. The data analysis of Fig. 8 allows us to determine the relationship between α_{A} and α_{M} with high accuracy. For the data of Fig. 8 equality (6) (and, also the condition $R_{\mathrm{Rem}} = R(H^*_{\mathrm{ini}})$) is executed with the following ratio: $\alpha_{\mathrm{M}} = 1.52\alpha_{\mathrm{A}} - 1.66$. It is unambiguous that $\alpha_{\mathrm{M}} \neq \alpha_{\mathrm{A}}$ and if we consider that the parameter α itself can reach values of the order of 12–25 [23,25–29,43,44], then

$$\alpha_{\mathrm{M}} > \alpha_{\mathrm{A}}. \quad (7)$$

The magnetization of a superconductor is due to two contributions opposite in sign: Meissner currents and Abrikosov vortices. Their contribution to the field in the intergranular medium is also different in sign, which can be seen, for example, from the representation of Fig. 6, if $\mathbf{M}_{\mathrm{G}}$ is alternately replaced by the magnetic moment from the Meissner current Mm, or from the Abrikosov vortices $\mathbf{M}_{\mathrm{A}}$. If the outer field increases and $\mathbf{H} \parallel \mathbf{Z}$, then $\mathbf{M}_{\mathrm{M}}$ is antiparallel , and $\mathbf{M}_{\mathrm{A}} \parallel \mathbf{Z}$. Then the lines of magnetic induction from vortices in the intergranular spaces have the opposite direction, and from Meissner currents — parallel to the external field direction [55]. The resulting inequality (7) implies a different effect of the trapped flux and Meissner currents on the effective field in the intergranular medium. In other words, „one gauss“ from Meissner currents leads to greater resistance in an intergranular medium than „one Gauss“ from Abrikosov vortices.

You can specify one of the possible reasons leading to the inequality (7). Although the investigated HTS of the yttrium system has significantly less anisotropy of the critical current (and, accordingly, the diamagnetic signal) than the HTS of the bismuth system, the ratio of critical currents along the c-axis J_{Cc} and in the $a-b$ plane $J_{\mathrm{Ca}-b}$ for yttrium HTS is not small: $J_{\mathrm{Ca}-b}/J_{\mathrm{Cc}} \sim 4-8$ [52,56,57]. In this case, the Meissner currents $J_{\mathrm{Ma}-b}$ flowing in $a-b$ planes significantly exceed the Meissner currents J_{Mc} flowing in planes parallel to the axis c [58]. The magnetization recorded in magnetic measurements (this is the projection of magnetization on the axis **Z**, see Fig. 6) of a granular HTS sample shows a certain averaged over all magnetic moments from the currents $J_{\mathrm{Ma}-b}$ and J_{Mc} value (with taking into account that the crystalographic axes c of the granules are located chaotically). However, locally magnetic moments (especially for currents $J_{\mathrm{Ma}-b}$) may have a stronger effect on intergranular intervals than is expected for the average value of magnetization.

Abrikosov vortices in granular HTS permeate many granules, and the vortices demonstrate complex dynamics depending on the magnitude of the field and temperature [59–61]. Inside anisotropic granules, vortices also tend to be located along the c-axis [53,57], that is, deviate from the direction of the external field. However, the plasticity of the vortex lattice can reduce this deviation. In our opinion, the effect of granule anisotropy on the value of M_{Rem} is insignificant. The different effect of the anisotropy of granules on Meissner currents and trapped vortices explains the inequality (7).

4. Conclusion

The hysteresis behavior of the magnetoresistance of granular HTS is accompanied by many interesting features, one of which is the presence of residual resistance R_{Rem} after exposure to an external magnetic field. The main attention in this work was paid to the influence of the external maximum applied field H_{max}, or, equivalently, the influence of the trapped flux on R_{Rem}. As a result of the analysis of the data obtained on the HTS sample $YBa_2Cu_3O_{7-\delta}$, we obtained the following results. It is shown that R_{Rem} clearly correlates with the magnitude of the residual magnetization of M_{Rem}. In this case, M_{Rem} is determined only by the magnetic flux trapped in the granules, and the corresponding dissipation, which determines the value of R_{Rem}, occurs only in the intergranular boundaries. The magnetoresistance of the HTS $YBa_2Cu_3O_{7-\delta}$ was also compared for two cases in which either only the Meissner state (diamagnetism) is realized in granules, or there is only a flux trapped in granules (in zero external field). This, taking into account the magnetization data, allowed us to determine the relationship between the parameters (α_{M} and α_{A}) characterizing the degree of condensation of the magnetic flux in the intergranular medium. In the effective field concept (expression (2)) it is the flux compression in the intergranular medium that determines most of the features of the behavior of the magnetoresistance of granular HTS. It turned out that the parameter α is different for Meissner currents and for the trapped flux (Abrikosov vortices), moreover, the inequality $\alpha_{\mathrm{M}} > \alpha_{\mathrm{A}}$ holds. In other words, a change in magnetization by „one gauss“

from Meissner currents makes a greater contribution to the effective field in an intergranular medium than a change in magnetization by „one Gauss“ from Abrikosov vortices. One of the reasons for the discovered fact may be the anisotropy of the superconducting properties of the HTS within a single granule, although, in general, the directions of the crystallographic axes of the granules (crystallites) in the granular HTS are distributed randomly. As a result, when describing the hysteresis of the magnetoresistance of a granular HTS, for an effective field in an intergranular medium, it must be taken into account that $\alpha_M > \alpha_A$. The obtained conclusion can be useful not only for explaining magnetotransport properties, but also important for analyzing the magnetic properties of granular superconductors with anisotropy.

Acknowledgments

The authors thank V.M. Sosnin, A.A. Krasikov for discussing the results, I.V. Nemtsev for electron microscopy of the sample, M.A. Pochekutov for assistance in conducting magnetotransport measurements.

Funding

The study was carried out with the financial support of the Russian Foundation for Basic Research, the Government of the Krasnoyarsk Territory, the Krasnoyarsk areaal Science Foundation within the framework of the scientific project No. 20-42-240008 „The effect of the introduction of paramagnetic ions of rare earth elements on the superconducting properties of materials based on YBCO“.

The study of the microstructure and magnetic measurements were carried out using the equipment of the Center for Collective Use of the FITC KNC SB RAS.

Conflict of interest

The authors declare that they have no conflict of interest.

References

[1] Pratima, S. Vats. J. Supercond. Nov. Magn. (2022). https://doi.org/10.1007/s10948-022-06206-8
[2] K. Jin, G. He, X. Zhang, S. Maruyama, S. Yasui, R. Suchoski, J. Shin, Y. Jiang, H.S. Yu, J. Yuan, L. Shan, F.V. Kusmartsev, R.L. Greene, I. Takeuchi. Nature Commun. **6**, 7183 (2015). https://doi.org/10.1038/ncomms8183
[3] M.A. Olutas, A. Kilic, K. Kilic, A. Altinkok. J. Supercond. Nov. Magn. **26**, 3369 (2013).
[4] V.V. Derevyanko, M.S. Sungurov, T.V. Sukhareva, V.A. Finkel', Yu.N. Shakhov. Phys. Solid State **59**, 229 (2017).
[5] X. Zhu, H. Yang, L. Fang, G. Mu, H.-H. Wen. Supercond. Sci. Technol. **21** (2008) 105001.
[6] A. Altinkok, K. Kilic, M. Olutas, A. Kilic. J. Supercond. Nov. Magn. **26**, 3085 (2013). https://doi.org/10.1007/s10948-013-2139-y
[7] A.A. Bykov, K.Yu. Terent'ev, D.M. Gokhfeld, N.E. Savitskaya, S.I. Popkov, M.I. Petrov. J. Supercond. Nov. Magn. **31**, 3867 (2018).
[8] K.A. Shaikhutdinov, D.A. Balaev, S.I. Popkov, M.I. Petrov. Supercond. Sci. Technol. **20**, 491 (2007).
[9] I. Pallecchi, C. Tarantini, Y. Shen, R.K. Singh, N. Newman, P. Cheng, Y. Jia, H.-H. Wen, M. Putti. Supercond. Sci. Technol. **31**, 034007 (2018). doi.org/10.1088/1361-6668/aaaaa6
[10] D.M. Gokhfeld, D.A. Balaev, S.V. Semenov, M.I. Petrov. Phys. Solid State **57**, *11*, 2145 (2015). DOI: 10.1134/S1063783415110128
[11] A. Palau, T. Puig, X. Obradors, E. Pardo, C. Navau, A. Sanchez, A. Usoskin, H.C. Freyhardt, L. Fernández, B. Holzapfel, R. Feenstra. Appl. Phys. Lett. **84**, 230 (2004). https://doi.org/10.1063/1.1639940
[12] D.A. Balaev, A.G. Prus, K.A. Shaukhutdinov, D.M. Gokhfeld, M.I. Petrov. Supercond. Sci. Technol. **20**, 495 (2007). https://doi.org/10.1088/0953-2048/20/6/002
[13] M.I. Eremets, V.S. Minkov, A.P. Drozdov, P.P. Kong, V. Ksenofontov, S.I. Shylin, S.L. Bud'ko, R. Prozorov, F.F. Balakirev, Dan Sun, S. Mozaffari, L. Balicas. J. Supercond.Nov. Magn. **35**, 965 (2022).
[14] I.A. Troyan, D.V. Semenok, A.G. Kvashnin, A.V. Sadakov, O.A. Sobolevskiy, V.M. Pudalov, A.G. Ivanova, V.B. Prakapenka, E. Greenberg, A.G. Gavriliuk, I.S. Lyubutin, V.V. Struzhkin, A. Bergara, I. Errea, R. Bianco, M. Calandra, F. Mauri, L. Monacelli, R. Akashi, A.R. Oganov. Adv. Mater. 2006832 (2021).
[15] L. Ji, M.S. Rzchowski, N. Anand, M. Tinkham. Phys. Rev. B **47**, 470 (1993). https://doi.org/10.1103/PhysRevB.47.470
[16] M.I. Petrov, D.A. Balaev, K.A. Shaikhutdinov, K.S. Aleksandrov. Supercond. Sci. Technol. **14**, 798 (2001). https://doi.org/10.1088/0953-2048/14/9/333
[17] G.L. Bhalla, Pratima, A. Malik, K.K. Singh. Physica C **391**, 17 (2003). https://doi.org/10.1016/S0921-4534(03)00805-0
[18] D. Lopez, R. Decca, F. de la Cruz. Supercond. Sci. Technol. **5**, 276 (1992). https://doi.org/10.1088/0953-2048/5/1S/061
[19] M. Prester. Supercond. Sci. Technol. **11**, 333 (1998).
[20] D.A. Balaev, S.I. Popkov, S.V. Semenov, A.A. Bykov, E.I. Sabitova, A.A. Dubrovskiy, K.A. Shaikhutdinov, M.I. Petrov. J. Supercond. Nov. Magn., **24**, 2129 (2011).
[21] D.A. Balaev, A.A. Dubrovskii, K.A. Shaykhutdinov, S.I. Popkov, D.M. Gokhfeld, Yu.S. Gokhfeld, M.I. Petrov. JETP **108**, 241 (2009). https://doi.org/10.1134/S106377610902006X
[22] D.A. Balaev, S.I. Popkov, S.V. Semenov, A.A. Bykov, K.A. Shaykhutdinov, D.M. Gokhfeld, M.I. Petrov. Physica C **470**, 61 (2010). https://doi.org/10.1016/j.physc.2009.10.007.
[23] D.A. Balaev, S.I. Popkov, E.I. Sabitova, S.V. Semenov, K.A. Shaykhutdinov, A.V. Shabanov, M.I. Petrov. J. Appl. Phys. **110**, 093918 (2011). https://doi.org/10.1063/1.3657775
[24] D.A. Balaev, A.A. Bykov, S.V. Semenov, S.I. Popkov, A.A. Dubrovskii, K.A. Shaykhutdinov, M.I. Petrov. Phys. Solid State **53**, 922 (2011). https://doi.org/10.1134/S1063783411050052
[25] D.A. Balaev, S.V. Semenov, M.I. Petrov. J. Supercond. Nov. Magn. **27**, 1425 (2014). https://doi.org/10.1007/s10948-014-2491-6
[26] D.A. Balaev, S.V. Semenov, M.A. Pochekutov. J. Appl. Phys. **122**, 123902 (2017). https://doi.org/10.1063/1.4986253
[27] S.V. Semenov, D.A. Balaev. Physica C **550**, 19 (2018). https://doi.org/10.1016/j.physc.2018.04.005

[28] S.V. Semenov, D.A. Balaev. J. Supercond. Nov. Magn. **32**, 2409 (2019). https://doi.org/10.1007/s10948-019-5043-2
[29] S.V. Semenov, D.A. Balaev. Phys. Solid State **62**, 1136 (2020). https://doi.org/10.1134/S1063783420070239
[30] T.V. Sukhareva, V.A. Finkel. J. Exp. JETP Phys. **107**, 787 (2008).
[31] V.V. Derevyanko, T.V. Sukhareva, V.A. Finkel'. Phys. Solid State **60**, 470 (2018).
[32] T.V. Sukhareva, V.A. Finkel. JETP Lett. **108**, 243 (2018).
[33] T.V. Sukhareva, V.A. Finkel. J. Low Temp. Phys. **44**, 194 (2018).
[34] T.V. Sukhareva, V.A. Finkel. J. Low Temp. Phys. **46**, 550 (2020).
[35] J. Barzola-Quiquia, S. Dusari, C. Chiliotte, P. Esquinazi. J. Supercond. Nov. Magn. **24**, 463 (2011). https://doi.org/10.1007/s10948-010-0973-8
[36] C. Tien, C.S. Wur, K.J. Lin, E.V. Charnaya, Yu.A. Kumzerov. Phys. Rev. B **61**, *12*, 14834 (2000).
[37] A.A. Shikov, M.G. Zemlyanov, P.P. Parshin, A.A. Naberezhnov, Yu.A. Kumzerov. Phys. Solid State **54**, 2345 (2012). https://doi.org/10.1134/S106378341212030X
[38] D.A. Balaev, A.A. Dubrovskiy, S.I. Popkov, K.A. Shaikhutdinov, O.N. Mart'yanovc, M.I. Petrov. J. Exp. JETP Phys. **110**, *4*, 584 (2010).
[39] J.E. Hirsh. J. Supercond. Nov. Magn. (2022). https://doi.org/10.1007/s10948-022-06340-3
[40] V.V. Derevyanko, T.V. Sukhareva, V.A. Finkel. Tech. Phys. **53**, 321 (2008). https://doi.org/10.1134/S1063784208030067
[41] T.V. Sukhareva, V.A. Finkel. Phys. Solid State **50**, 1001 (2008). https://doi.org/10.1134/S1063783408060012
[42] D. Daghero, P. Mazzetti, A. Stepanescu, P. Tura. Phys. Rev. B **66**, 11478 (2002). https://doi.org/10.1103/PhysRevB.66.184514
[43] S.V. Semenov, A.D. Balaev, D.A. Balaev. J. Appl. Phys. **125**, 033903 (2019). https://doi.org/10.1063/1.5066602
[44] D.A. Balaev, S.V. Semenov, D.M. Gokhfeld. J. Supercond. Nov. Magn. **34**, 1067 (2021). https://doi.org/10.1007/s10948-021-05812-2
[45] J. Jung, M.-K. Mohamed, S.C. Cheng, J.P. Franck. Phys. Rev. B. **42**, 6181 (1990).
[46] B. Andrzejewski, E. Guilmeau, C. Simon. Supercond. Sci. Technol. **14**, 904 (2001).
[47] F. Pérez, X. Obradors, J. Fontcuberta, X. Bozec, A. Fert. Supercond. Sci. Technol. **9**, 161 (1996).
[48] D.-X. Chen, R.W. Cross, A. Sanchez. Cryogenics **33**, *7*, 695 (1993). https://doi.org/10.1016/0011-2275(93)90022-G
[49] D.M. Gokhfeld. Phys. Solid State **56**, 2380 (2014). https://doi.org/10.1134/S1063783414120129
[50] D.M. Gokhfeld. Tech. Phys. Lett. **45**, 1 (2019). https://doi.org/10.1134/S1063785019010243
[51] C. Böhmer, G. Brandstätter, H.W. Weber. Supercond. Sci. Technol. **10**, A1 (1997).
[52] R. Liang, P. Dosanjh, D.A. Bonn, W.N. Hardy, A.J. Berlinsky. Phys. Rev. B **50**, *7*, 4212 (1994).
[53] G. Blatter, M.V. Feigel'man, V.B. Gekshkebein, A.I. Larkin, V.M. Vinokur. Rev. Mod. Phys. **66**, 1125 (1994). https://doi.org/10.1103/RevModPhys.66.1125.
[54] D.H. Liebenberg, R.J. Soulen, T.L. Francavilla, W.W. Fuller-Mora, P.C. McIntyre, M.J. Cima. Phys. Rev. B **51**, 11838 (1995). https://doi.org/10.1103/ PhysRevB.51.11838
[55] S.V. Semenov, D.M. Gokhfel'd, K.Yu. Terent'ev, D.A. Balaev. Phys. Solid State, **63**, *12*, 1785 (2021). DOI: 10.1134/S1063783421100334
[56] A. Umezawa, G.W. Crabtree, J.Z. Liu, T.J. Moran, S.K. Malik, L.H. Nunez, W.L. Kwok, C.H. Sowers. Phys. Rev. B **38**, *4*, 2843 (1988).
[57] S.J. Bending, M.J.W. Dodgson. J. Phys.: Condens. Matter **17**, R955 (2005). DOI: 10.1088/0953-8984/17/35/R01
[58] D.M. Gokhfeld, D.A. Balaev. Phys. Solid State **62**, *7*, 1145 (2020). DOI: 10.1134/S1063783420070069
[59] M.R. Koblischka, S.P. Kumar Naik, A. Koblischka-Veneva, M. Murakami, D.M. Gokhfeld, E.S. Reddy, G.J. Schmitz. Materials **12**, *6*, 853 (2019). https://doi.org/10.3390/ma12060853
[60] M.R. Koblischka, S.P. Kumar Naik, A. Koblischka-Veneva, D.M. Gokhfeld, M. Murakami. Supercond. Sci. Technol. **33**, *4*, 044008(2020). https://doi.org/10.1088/1361-6668/ab72c3
[61] Y. Yeshurun, A.P. Malozemoff, A. Shaulov. Rev. Mod. Phys. **68**, 911 (1996). https://doi.org/10.1103/RevModPhys.68.911

Editor K.V. Emtsev